JPMTR 117 | 1821
DOI 10.14622/JPMTR-1821
UDC 655:577.1+577.2-035.67|542.9-9

Original scientific paper
Received: 2018-12-09
Accepted: 2019-01-30

A test system for the printing of functional nucleic acids onto different carriers and verification of its functionality by DNA dyes

Jacqueline Stamm[1], Dieter Spiehl[1], Jeannine Jaeger[2], Florian Groher[2], Tobias Meckel[3], Beatrix Suess[2] and Edgar Dörsam[1]

[1] Institute of Printing Science and Technology, Technische Universität Darmstadt, Magdalenenstraße 2, 64289 Darmstadt — stamm@idd.tu-darmstadt.de, spiehl@idd.tu-darmstadt.de
[2] Department of biology, synthetic genetic circuits, Technische Universität Darmstadt, Schnittspahnstraße 10, 64287 Darmstadt — jaeger.jea@bio.tu-darmstadt.de, groher@bio.tu-darmstadt.de, bsuess@bio.tu-darmstadt.de
[3] Macromolecular and Paper Chemistry, Technische Universität Darmstadt, Alarich-Weiss-Straße 8, 64287 Darmstadt — meckel@cellulose.tu-darmstadt.de, doersam@idd.tu-darmstadt.de

Abstract

The creation of inkjet printed biosensors belongs to rising applications of functional printing. One of their many uses is the detection of antibiotic residues in milk or meat from food-producing animals, which have been excessively treated. For example, they are treated with the fluoroquinolone ciprofloxacin (CFX), which we want to detect with an aptamer-based fluorescence biosensor, printed onto a carrier material. For that purpose, inkjet printing and several carrier materials are analyzed in their ability to obtain the functionality of nucleic acids. The printing process is analyzed by characterizing DNA and buffer solutions and by comparing printed with unprinted DNA using an agarose-gel test. The carrier materials are preselected by analyzing the auto-fluorescence excitation and emission spectra of ten different materials out of which three with the lowest intensity at the CFX excitation and emission peaks are chosen. After printing with DNA onto these materials, the fluorescence induced with DNA dyes is measured. The experiments show that nucleic acids can be inkjet printed without damage and that many foils and papers commonly used in the laboratory show auto fluorescence when excited in the UV-spectrum. Other properties of the carrier materials are important as well. Here a selection containing the paper Whatman Grade 1, the foil Hostaphan GUV 4600 and the nitrocellulose HF 120 are compared in their ability to sustain the functionality of nucleic acids printed onto them. Although, we were able to select a suitable material for future experiments of printing a CFX-biosensor, there are still open questions concerning the interactions between nucleic acids and different carrier materials.

Keywords: inkjet, aptamers, fluorescence, ciprofloxacin, biosensor

1. Introduction and background

In printing technology and research, the focus is shifting from graphic arts to functional printing. For example, printed circuits (Pankalla, et al., 2013), antennas (Mohassieb, et al., 2017) or gravure printed organic light emitting diodes (Raupp, et al., 2017) or transistors (Spiehl, et al., 2015) are current areas of research and some of them are already applied in production of goods. Another application are printed biosensors, which find use in the fields of health (Song Xu and Fan, 2006), food safety (Alocilja and Radke, 2003), environment protection (Justino, Duarte and Rocha-Santos, 2017) or even homeland security (Joshi, et. al., 2006). A biosensor is a device consisting of three parts: the bioreceptor, which binds to the target molecule; the transducer, which transforms the interaction into a measurable signal; and the signal processor, which displays the result in a user-friendly way (Kivirand, Kagan and Rinken, 2013). Concrete examples for biosensor application are the detection of pathogens to monitor and contain the spread of serious illnesses (Ecker, et al., 2008), determination of blood glucose levels for diabetics (Wang, 2001), controlling the usage of dangerous insecticides

(Bachmann and Schmid, 1999), which are also linked to the death of bees (Brandt, et al., 2016) or the detection of toxins, pesticides and antibiotic residues in foods (Mello and Kubota, 2002). In this paper special interest is given to the antibiotic residues in food-producing animals.

Antimicrobial drugs are used on food-producing animals for therapeutic, prophylactic or growth promoting purposes. They include disinfectants, antiseptics and antibiotics. It is an almost inevitable consequence that bacteria constantly exposed to antibiotics become resistant and the antibiotics ineffective. Since 1990 the resistance and particularly multiple resistance to several antibiotics has increased drastically in developed countries leading to numerous outbreaks of serious diseases (Threlfall, et al., 2000). In fact, antibiotic resistance is known to be one of the main public health problems (Novais, et al., 2010). Most antibiotics used are sulfonamides (20 %) or fluoroquinolones (19 %), followed by aminoglycosides (15 %), phenicols (15 %), β-lactams (15 %), tetracyclines (8 %) and oxazolidinones (8 %) (Cháfer-Pericás, Maquieira and Puchades, 2010). One example is the fluoroquinolone ciprofloxacin (CFX), which is used to treat a wide variety of bacterial infections on animals and humans (Groher and Suess, 2016; Groher, et al., 2018; Jaeger, et al., 2019).

Currently established methods of detecting antibiotics can be divided into two groups. Most frequently used are confirmatory methods, generally involving mass spectrometry. They are, however, time consuming, expensive and require specific equipment as well as training. Second are screening methods such as microbiological assays and immunoassays. While microbiological assays lack specificity and require long incubation times, immunoassays require the *in vivo* production of antibodies and are restricted in possible targets to antigens. The development of other screening methods is increasing considerably, with biosensors taking up about 8 % of all used methods (Cháfer-Pericás, Maquieira and Puchades, 2010). The possibility for a new biosensor method has arisen twenty years ago with the development of synthetic aptamers.

We have developed a CFX-binding ribonucleic acid aptamer (RNA-aptamer). Aptamers are approx. 25–100 nucleotide-long deoxyribonucleic acid aptamer (DNA) or RNA that bind specifically to molecular targets. They possess a complex three-dimensional structure, which entwines around its specific target, its ligand, upon binding (Garst, Edwards and Batey, 2011). Other interactions are also involved in recognizing the target molecule (Edwards, Klein and Ferré-D'Amaré, 2007). Additionally, aptamers can be denatured reversibly. This means that changing the surrounding conditions will only cause aptamers to temporarily unfold, while – upon returning to the original binding conditions – they are able to regain their functionality (McKeague and DeRosa, 2012). The in vitro procedure of generating aptamers enables a great control over the binding conditions and the target selection. They can be generated de-novo for a specific ligand via a procedure called systematic evolution of ligands by exponential enrichment (SELEX). Usually 6 to 20 cycles of this procedure are needed (Ellington and Szostak, 1990).

Our motivation is the creation of a printed aptamer-based biosensor for the detection of CFX. There are mainly four components to consider when developing a printed biosensor: the ink formulation, the printing process, the carrier material and the readout. The ink formulation has to include the bioreceptor, namely the CFX-binding aptamer, as-well as the transducer, which produces the signal. In this case the transducer is already included, because the autofluorescence of CFX is reduced automatically after binding with its aptamer. For other antibiotics an element, which transforms the binding process into a signal, would have to be included.

In this paper, the focus is on analyzing general printing experiments of nucleic acids. For this purpose, a model system is used instead of the aptamer. The aptamer is time-consuming in production and will be printed after the investigations described in this work. The bioreceptor consists of a printed nucleic acid and the transducer is a special dye, applied afterwards. If the nucleic acid is still functional the dye is able to insert itself into the sequence and an increase in fluorescence can be detected. The requirements for the printing process are the delivery of small quantities of functional material in the liquid phase into well-defined locations. We will confirm, that inkjet printing is suitable for this job in 3.1, although each printhead has only a narrow viscosity range and exercises a high mechanical shear onto the used ink. Finally, a carrier material has to be found, which can store and protect the printed aptamers, without inhibiting its functionality or interfering with the produced signal and altering the readout.

In the presented tests, experience is gathered in handling and printing nucleic acids as well as their behavior on different carrier materials on the example of DNA. Parts of this work were already presented at the 45th International iarigai Conference in Warsaw (Stamm, et al., 2018). The end goal is to transfer the gained knowledge into the printing of RNA-aptamer biosensors.

2. Materials and methods

All materials and methods used for creating, characterizing and evaluating the DNA biosensor model system are introduced in the following sections. First, the DNA ink is presented, as well as the DNA dyes, followed by

the ink characterization. Then a suitable printing process and carrier materials are chosen. Finally, the different equipment used for fluorescence detection and their application areas are explained.

2.1 DNA and DNA dyes

Deoxyribonucleic acid is a pair of polynucleotide biopolymer strands that form a so-called double helix, while ribonucleic acid is a single strand of said polymer. The DNA dyes are used to make DNA visible. They intercalate in the DNA, meaning they insert themselves between the bases and increase their fluorescence after excitation. This principle is used as model detector system in this work, for the detection of DNA printed onto a carrier. The experiments mentioned and shown here use Hoechst 33342 (Thermo Fisher Scientific, Waltham, MA, USA), because of its similar fluorescence excitation and emission spectra to CFX (Figure 1); and YOYO-1 iodide (Thermo Fisher Scientific, Waltham, MA, USA), because of its significantly higher intensity increase after intercalating (Figure 2). The excitation and emission spectra are shown at the end of this section while introducing the fluorescence measuring equipment.

There are three different kinds of DNA we use for different experiments: DNA with low relative molecular mass (M_r = 1.3 to 7.9 million g/mol), DNA V11 and a plasmid solution. Their properties and usages are listed in Table 1. The DNA low M_r is chosen because its molecular mass is comparable to that of the CFX aptamer. The difference in molecular structure has no great impact on the macroscopic fluid properties. When doing the DNA staining, the DNA V11 is used because of its comparable structure. Eventually the plasmid with its high molecular mass and circular structure is used for testing of potential damaging during printing, because it is even more sensitive to damage than the CFX aptamer. All of them are stored and used in buffer solution, which consists of water from the Milli-Q processing plant, 40 mM of the chemical buffer agent HEPES, 125 mM potassium chloride and 5 mM magnesium chloride.

2.2 Fluid characterization

Nucleic acids, stored in their buffer, form the ink that needs to be printed to create a biosensor. But different printing processes call for different ink properties. Usually the restricting properties are the viscosity and the surface tension, which requires the knowledge of the density as well.

The viscosity can be determined using the rotational rheometer Panalytical Kinexus lab+ by Malvern. The fluid is inserted into a gap between a plate and a variable cone, called the geometry. The geometry with 60 mm diameter and 1° inclination is suitable for low viscous fluids and is used in the following characterization. By rotating the cone with increasing speed (10 s^{-1} to 1000 s^{-1} was used), the shear rate onto the fluid is increased and the resulting shear stress is measured. The viscosity is then found by the slope of a linear fit to shear stress over shear rate.

The surface tension can be measured with the tensiometer DSA 100 from Krüss. Droplets are created either hanging from the syringe (pendant) or set down onto a surface (sessile) and their shape is analyzed regarding their curve and contact angle respectively. The general surface tensions are measured via pendant drops, whereas their polar and disperse ratios via sessile drops onto a known material, here Teflon.

Finally, the density can be determined with a pycnometer. The glass flask has a well-defined filling capacity and is used by measuring the weight of an unknown substance in reference to a substance with known density, here water.

2.3 Printing methods and carrier materials

The established printing processes can be divided into conventional printing, which requires a printing plate, and non-impact printing (Kipphan, 2001). Considering the requirements of transferring small amounts of nucleic acids in a clean environment, one option of each group seems most promising: gravure and inkjet printing. In both methods, it is possible to have all machine parts coming into contact with the ink made from inert materials like polytetrafluoroethylene (PTFE), polyproylene (PP), chromium, stainless steel or silicone.

We will focus on inkjet printing because of its more variable dispensing options when doing a development process in the lab.

Table 1: The used DNA solutions with their properties and applications; all of them are stored in buffer solution and used in their liquid state

Name	Properties	Usage
DNA low M_r	Salmon sperm, low priced	Analyzing fluid properties
DNA V11	R10K6_V11 as DNA	Functional tests
Plasmid	Circular DNA	Shear force stress test

Table 2: The materials initially chosen as possible carriers to print on, listed with the manufacturer and material general name

Specific name	Manufacturer	Material	Thickness
Hostaphan GN 4600	Mitsubishi Polyester Film	Polyethylene therephthalate (PET)	125 µm
Hostaphan GUV 4600	Mitsubishi Polyester Film	Polyethylene therephthalate (PET)	50 µm
Melinex 339	DuPont Teijin Films	Polyethylene therephthalate (PET)	250 µm
Melinex Q65FA	DuPont Teijin Films	Polyethylene naphthalate (PEN)	125 µm
SyntiTec 3900	Sihl Direct	Polypropylene (PP)	180 µm
SFT 40 T	Taghleef Industries	Biaxially oriented polypropylene (BoPP)	40 µm
Rotilabo 601	Carl Roth	Paper	160 µm
Whatman Grade 1	GE Healthcare	Paper	180 µm
Amersham Hybond RPN2020N	GE Healthcare	Nylon membrane	160 µm
HF 120	Millipore	Nitrocellulose	230 µm

The used inkjet printer Autodrop from Microdrop Technologies is equipped with piezo-based drop-on-demand single nozzle printheads. They consist of glass nozzles with different available orifice diameters in the range of 30 µm to 100 µm. Prior to printing the ink is filtrated using a polyethersulfone (PES) filter, with a pore size of 0.2 µm. Afterwards the nozzle and inflow need to be cleaned. Long purging cycles, that pass several milliliters of water or sodium hydroxide, ensure that no molecules remain in the flow that could clog the nozzle after drying out.

Ten different carrier materials were initially chosen from the categories paper, plastic and combinations of both. Their names are listed in Table 2 together with the manufacturer and material general name. In the text carrier materials are called by their specific name.

2.4 The readout

Two devices are used for fluorescence detection. For fluid measurements the microplate reader CLARIOstar by BMG LABTECH is chosen, as it allows for precise recordings of both excitation and emission spectra measured in reflection. However, the device records the spectral properties of each sample on a single point, making it suitable for measurements of homogeneous fluids but not for potentially inhomogeneous solid samples. For inhomogeneous solid samples a space-resolved imaging method is needed given by the imager Fusion FX Edge from Vilber. The imager has set illuminations for excitation and filter for emission, which need to be chosen according to the inspected substance. Another limitation is the fixed position of the illumination and detection elements. The detected intensities are captured by a camera from above, while the LEDs, which emit in the visible spectrum, are also placed above and enable measurements in reflection mode. But the UVB illumination is placed below and only permits measurements in transmission. Based on the CFX spectra obtained by the microplate reader and the DNA dye spectra taken from the Thermo Fisher website (Hoechst, n.d.; YOYO-1, n.d.), the optimal combination of light source and emission filter is chosen to achieve the best sensitivity. The CFX and Hoechst 33342 are best excited by the UVB transillumination, which emits light with a peak at 312 nm. Its range lies mostly between 280 nm and 360 nm, but reaches up into the visible range. A cut is set at 400 nm by an additionally integrated filter. The best suited emission filter for CFX and Hoechst 33342 detection is filter F440, with a range of 470–590 nm (Figure 1). The fluorescence of CFX is measured in solution in the microplate reader, and the fluorescence of Hoechst 33342 is taken from Hoechst (n.d.). The CFX data

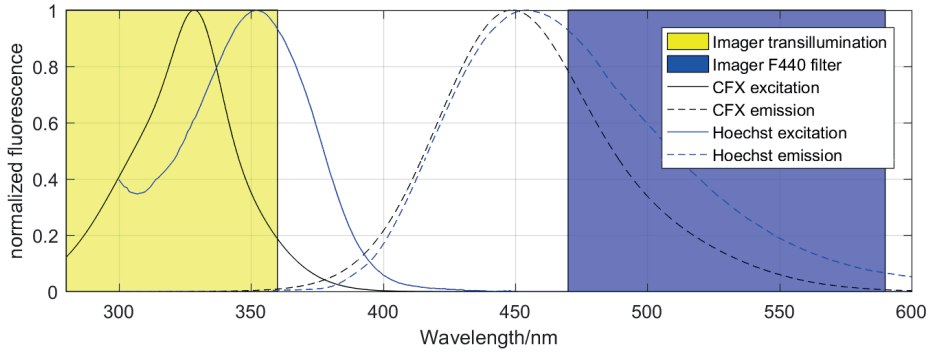

Figure 1: Excitation and emission spectra of the DNA dye Hoechst 33342 in comparison to CFX and the best fitting imager illumination and emission filter; the normalized fluorescence intensities are given over the wavelengths in nm

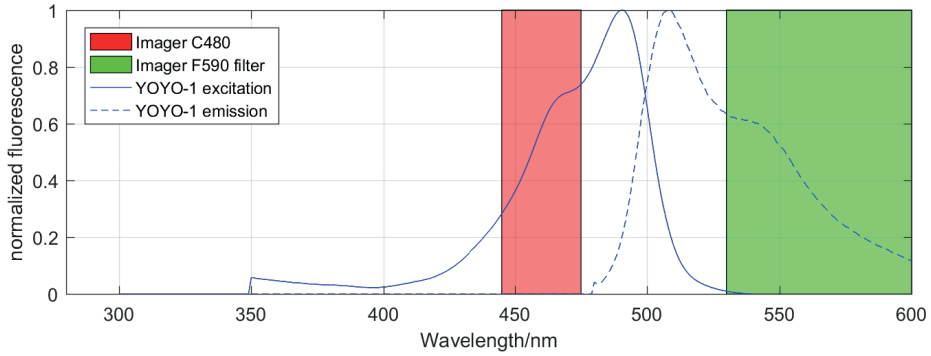

Figure 2: Excitation and emission spectra of the DNA dye YOYO-1 and the best fitting imager illumination and emission filter; the normalized fluorescence intensities are given over the wavelengths in nm

is extrapolated below 320 nm with a two term Gaussian fit. For the excitation of YOYO-1 the epi-illumination with an LED with 460 nm ± 15 nm (approx.) is used, which illuminates the sample from above. For the detection of YOYO-1 the filter F-590 fits best, which passes through 530–600 nm wavelengths (Figure 2). Spectral data were taken from YOYO-1 (n.d.).

3. Results and discussion

Two kinds of experiments are carried out. One concerning the maintenance of functionality during the printing process itself and one on sustaining the functionality on the carrier material. Both rely on fluorescence measurements.

3.1 Inkjet printing of nucleic acids

We need to verify that the used inkjet printer and its piezo-electric printhead are suitable for printing nucleic acids that are stored in their buffer solution. There are two main challenges to consider: ink printability and preservation of functionality. Each printhead has a range of ink surface tension and viscosity that have to be met to realize drop creation. In graphic arts insufficient properties can be compensated with additives. The surface tension can be lowered by adding surfactants like Triton X-100 or by adding solvents with lower surface tension like dimethyl sulfoxide. The viscosity can be raised by adding high viscous solvents like glycerol or ethylene glycol or polymers like sodium carboxymethyl cellulose, polyvinyl alcohol, or polyethylene glycol. But in functional printing the additive's effect on the functional material would have to be analyzed first. Usually inkjet printers operate in a region of 20 mN/m to 70 mN/m for the surface tension and 0.3 mPa·s to 100 mPa·s for the viscosity. For the used orifice diameter of 70 µm in the inkjet printer Autodrop, the viscosity should be between 0.4 mPa·s and 20 mPa·s. A surface tension range is not stated, but is expected to be at the upper end for general inkjet printers, because of the rather big drop volume of approx. 260 pl. The drop spacing can be varied to create different volume per area concentrations. The driving voltage of the printhead is set to 68 V, the pulse length is 24 µs and the frequency is 100 Hz.

The functionality of aptamers can be reduced in several ways during the printing process. First, the high mechanical shear of the piezo-electric printhead may rip the molecules apart. Second, nucleic acids are usually stored cool but in an inkjet printhead temperatures can rise during printing. Both, the printability and preservation of functionality, will be analyzed in the following.

First the DNA with low M_r and single fold concentrated buffer are characterized in comparison to water. The density is determined with a pycnometer, the surface tension is measured with a tensiometer and the viscosity is determined using a rotational rheometer. Density and surface tension are measured at 23 °C, the viscosity at 25 °C. The results are shown in Table 3.

Table 3: Fluid characterization of water, buffer and DNA low M_r in buffer, concerning the density, surface tension (ST) and viscosity; the densitiy of water is taken from literature as a reference

	Water	**Buffer**	**Buffer + DNA low M_r**
Density in g/ml	0.997541	1.00 ± 0.02	1.01 ± 0.02
ST in mN/m	70 ± 5	68 ± 4	70 ± 4
ST disperse	30 ± 5	28 ± 4	33 ± 5
ST polar	40 ± 8	40 ± 6	36 ± 6
Viscosity in mPa·s	0.90 ± 0.01	0.92 ± 0.01	0.93 ± 0.01

Within their measurement errors all fluids have the same properties and lie within the stated range of the used inkjet printhead. It is assumed that all printing techniques suitable for water should also work with nucleic acid solutions and first printing tests show no problems.

Whether the molecules are damaged during inkjet printing, is tested with a plasmid solution. One part (reference sample) of the solution is kept at the Biology department, another is transported and stored, and the last part is printed. The printing was done over several minutes at a constant position into a test tube to collect 200 µl. An agarose-gel assay test shows the size distribution of the added molecules by applying a voltage. The positions of the travelled molecules are made visible with dyes. The smaller the molecule is, the further it travels in the gel, compared to molecules with the same charge. The size of the band for a particular size gives a qualitative information about the amount of that molecule in the added solution. Figure 3 shows no difference in the molecular sizes of all three solutions. It is concluded, that the shear stress and heat from inkjet printing do not tear plasmid molecules apart and it is assumed, that it will not damage similar molecules such as aptamers. This is also suggested by other works on inkjet printing of DNA micro-arrays (Goldmann and Gonzales, 2000), fabricating microfluidic paper-based analytical devices (Yamada, et al., 2015), and depositing nucleic acids to fabricate DNA chips (Okamoto, Suzuki and Yamamoto, 2000).

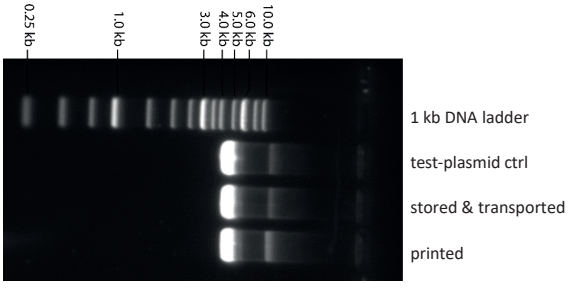

Figure 3: Plasmid test with 1 % agarose-gel, where the stored, transported and printed solutions can be seen in comparisson to a DNA ladder, which is used as a reference; per lane, 500 ng are applied

3.2 Functionality of nucleic acids printed onto carrier material

After verifying the printing process, the carrier material has to be chosen. We consider two aspects. First, the material properties should not interfere with the detection. Mainly this concerns the autofluorescence of the potential carrier material. Additionally, the carrier materials have to interact in a way that the nucleic acids are well stored and protected, but not hindered to bind. This can only be determined by testing.

3.2.1 Fluorescence of carrier materials

As we need to detect fluorescence for CFX or DNA dyes with a comparable fluorescence, the autofluorescence of the material has to be as low as possible in the same region. To determine which carrier material has the lowest auto-fluorescence in the range of the illumination and detection wavelength of CFX, all materials listed in Table 2 are examined at the maximum excitation and emission wavelength of CFX by an illumination at 328 nm and a detection at 450 nm, respectively. The measurements are carried out with punched-out pieces of the materials placed in a microplate and the fluorescence intensities measured in relative fluorescence units (RFU) by the plate reader are shown in Figure 4 in logarithmic scale to illustrate the broad range in intensities. It is not standard practice to analyze solid samples with a microplate reader, but the resulting order is confirmed by the imager measurements.

Especially certain plastics but also paper, because of its lignin content, show a high fluorescence. The intensity seems to correlate with their thicknesses as seen by the three PET foils Hostaphan GUV 4600, GN 4600 and Melinex 339.

Three different carrier materials with least fluorescence are selected for further experiments: the nitrocellulose HF 120, the PET Hostaphan GUV 4600 and the paper Whatman Grade 1. The PET foil was chosen over the BoPP foil SFT 40 T, because the latter is only produced in unpractically thin films.

Other works on depositing biological inks use nitrocellulose and nylon membrane (Goldmann and Gonzales, 2000) or filter paper and chromatography paper (Yamada, et al., 2015). There, the paper materials are stated to be composed of pure cellulose without additives such as brighteners, which might interfere with fluorescence-based detection, but the already mentioned lignin in paper has an autofluorescence, too. The filter paper Whatman Grade 1 is made of cotton fibers, which have a low lignin content when compared to other cellulose sources (Ververis, et. al., 2004).

3.2.2 Fluorescence of printed DNA and DNA dyes

Hoechst 33342 has the most similar fluorescence spectrum to CFX and seems promising to function as an alternative system for doing pre-tests for printing of aptamers and detection of CFX. Measurements in solution using the microplate reader, averaged over three measurements, show the characteristic rise and saturation of fluorescence when increasing the DNA concentration while holding the amount of 178 nM Hoechst 33342 constant (Figure 5).

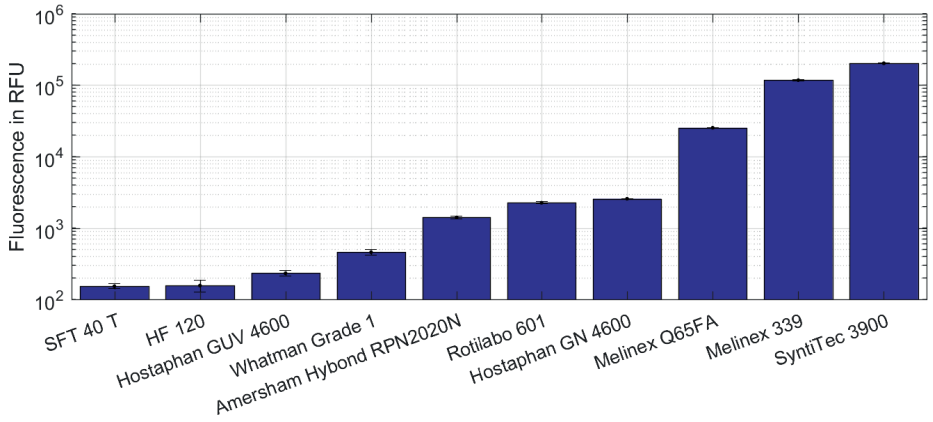

Figure 4: Fluorescence of the different carrier materials at CFX excitation (328 nm) and emission maxima (450 nm) taken with the microplate reader and shown in logarithmic scale

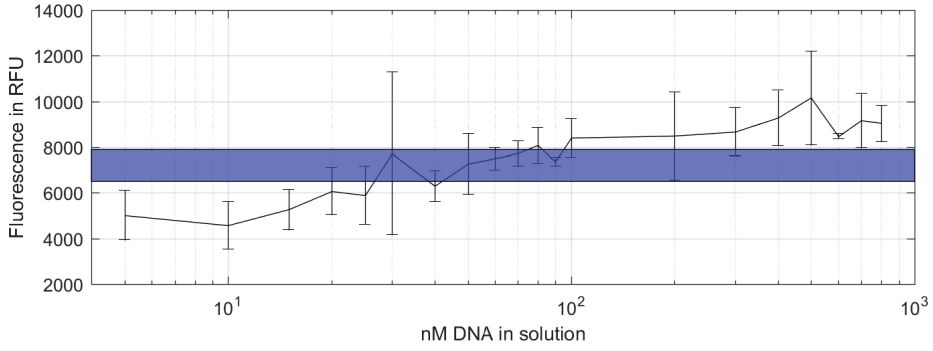

Figure 5: Fluorescence of different DNA V11 concentrations mixed with a constant amount of 178 nM Hoechst 33342 dye; the intensity of the dye alone is indicated by the blue bar

The problem is the relatively high fluorescence of the DNA dye alone when no DNA is present, which lies at 7200 ± 700 RFU and correlates with the intensity achieved by adding 30–90 nM DNA. All lower DNA concentrations added, actually yield a smaller fluorescence. The fluorescence intensity of Hoechst 33342 bound to DNA is not even twice the intensity of the unbound one, which was not expected, as the literature claims a twentyfold increase after binding. This is probably the case because DNA dyes are usually used with gel assays or inside cells, where the DNA concentration is a lot higher than in the tested solutions in the range of 1 nM to 1 µM. Furthermore, gels or assays are washed after staining to have only the dyed DNA left for detection.

Nonetheless the experiment is conducted with Hoechst 33342, since different DNA concentrations can be distinguished by fluorescence. A solution containing 10 µM DNA is printed onto the three selected carrier materials and left to dry, using the parameters in Table 4. Onto the same spots 5 µl solutions of different Hoechst 33342 concentrations, namely 10 nM, 100 nM, 1 µM, and 10 µM, are pipetted and the fluorescence is measured with the imager in the wet state (Figure 6).

Table 4: Inkjet printing parameters for four 0.5 cm × 0.5 cm squares with increasing DNA concentration, printed with a drop volume of 260 pl from a 10 µM DNA solution

Drop spacing	Grid size/ drops	Amount of DNA solution printed	
1.180 mm	6 × 6	0.2 ml/m²	0.01 µl
0.354 mm	20 × 20	2.0 ml/m²	0.10 µl
0.114 mm	62 × 62	20.0 ml/m²	1.00 µl
0.036 mm	196 × 196	20.0 ml/m²	10.00 µl

Table 5: The molar ratios between DNA and dye, where the DNA solution is concentrated by using varying amounts of a 10 µM solution; the dye is always used in 5 µl quantities, but of varying molar concentrations

Dye \ DNA	0.01 µl	0.1 µl	1 µl	10 µl
10 µM	0.002	0.02	0.20	2
1 µM	0.020	0.20	2.00	20
100 nM	0.200	2.00	20.00	200
10 nM	2.000	20.00	200.00	2000

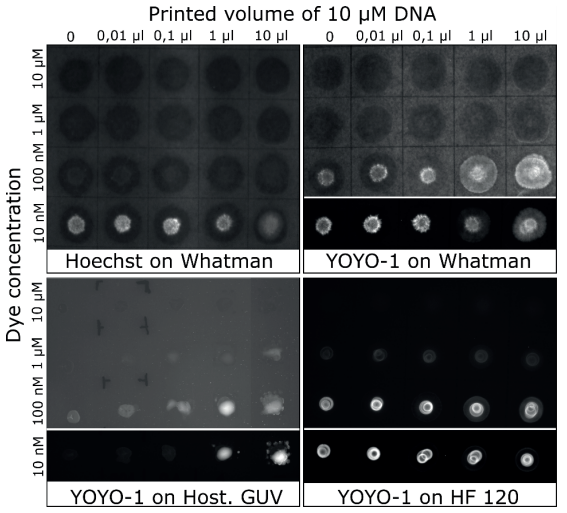

Figure 6: Different DNA volumes printed onto different carrier materials, abbreviated with Whatman (Whatman Grade 1), Host. GUV (Hostaphan GUV 4600); Hoechst stands for the dye Hoechst 33342

The dyes, varying in concentration, are added onto the dried DNA spots. All shown sub-pictures are taken with different exposure times to avoid over- and underexposure. All measurements are done when the spots are still wet after adding the dye. This yields 16 measurements for each carrier material with varying molar ratios between DNA and dye. The values lie between 0.002 and 2 000 and are shown in Table 5.

Unfortunately, all materials containing foils filter out the UVB transillumination, leaving only the paper as possible carrier. The intensity evaluation of Figure 6 is done by comparing area integrated densities and is shown in Figure 7. For each data set the integrated densities are processed by subtracting the dye fluorescence without DNA and normalizing to the highest fluorescence of that set. On Whatman Grade 1 the integrated intensity of the wet area increases between zero, 0.01 and 0.1 µl DNA solution, but falls to its initial value at 1 and 10 µl DNA. The only difference between low and high DNA concentration is that the fluorescence of the latter is spread more evenly instead of accumulating in the middle, see top left in Figure 6.

Hence, the DNA dye YOYO-1 is chosen as an alternative to Hoechst 33342 because of the fact that it is stated to have an enormously larger difference in fluorescence between the bound and unbound state. Due to the dif-

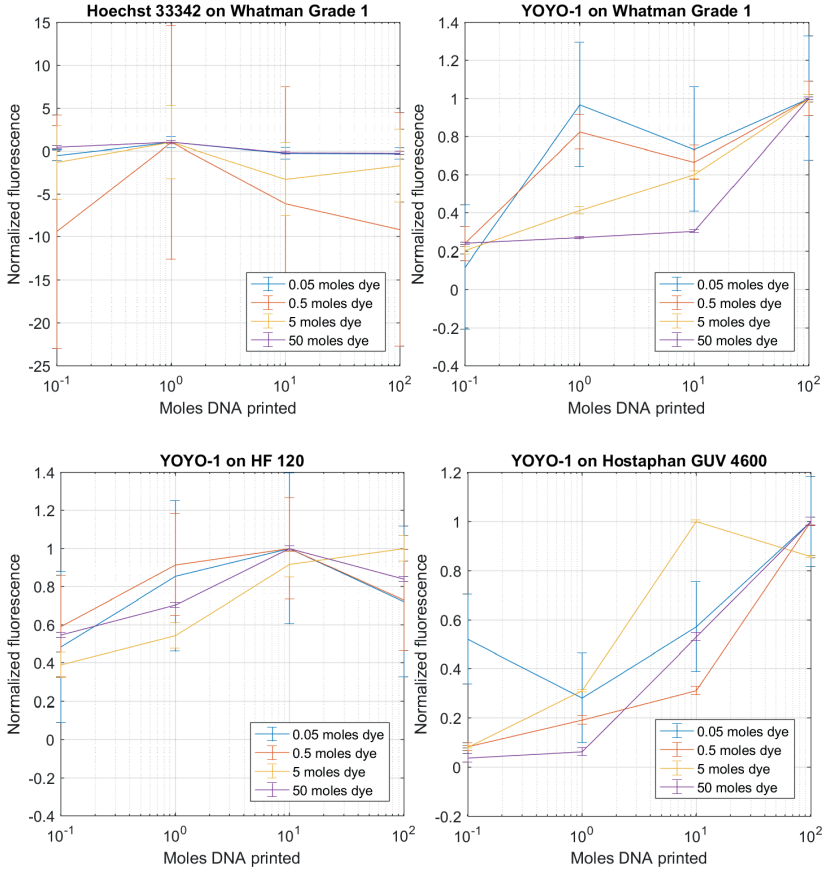

Figure 7: The intensity evaluation of Figure 6 with the fluorescence intensities of each data series normalized by setting the highest intensity to 1; straight lines are added in between single data points as guide for the eyes

ferent excitation wavelength, a different illumination can be chosen. As this illuminates from the top side, all three carrier materials can be used for this test.

The best results (Figure 6) are obtained with YOYO-1 on Whatman Grade 1 and Hostaphan GUV 4600. The fluorescence intensity (Figure 7) increases mostly for bigger DNA amounts. They are distinguishable from each other by their fluorescence while using all but the lowest dye concentration, however, the foil is impractical and not suited as carrier material for a biosensor. The wet spots are not well located, but spread unpredictably and are prone to running off the sample. On the nitrocellulose HF 120 a less steep increase in fluorescence is visible, but with a decrease towards the highest DNA concentration.

One important result of interactions between the printed nucleic acids and their carrier materials is their immobilization potential. The ink should not undergo global motion after adsorption and stay at the printed location, but it has to be able to undergo recognition and signaling chemistry (Carrasquilla, et al., 2015). One aspect that influences the immobilization is the protein binding capacity, which is assumed to be the highest for the nitrocellulose and the smallest for the foil. It is observed, that the general spreading of the printed fluid is the greatest on Whatman Grade. This is why it was suspected, that less of the DNA would be available for intercalation. But these factors prove to be less significant than the optimal immobilization potential of the filter paper.

A work on detecting viruses in dried serums, compares Whatman Grade 1, nylon membrane and nitrocellulose membrane as possible carrier materials and comes also to the conclusion, that Whatman Grade 1 provides the most efficient immobilization (Wang, Giambrone and Smith, 2002). The distribution of the DNA over the PET foil (Hostaphan GUV 4600) is nonuniform due to the creation of big droplets on its surface during printing and developing nonuniform contact lines during drying. Another aspect which should have an influence on the immobilization and thus the function of molecules on the substrates and especially on inhomogeneity of the fluorescence is the surface energy and its distribution over the substrate. This should be measured and compared to the obtained results.

4. Conclusions

On our way to printing a functional biosensor with aptamers we were able to answer a few questions. Inkjet printing is a suitable method for transferring variable amounts and concentrations of nucleic acid solutions without damaging the molecules. The work with fluorescence substances which require excitation in the central UVB sector identified several problems to consider in the future. The CFX and Hoechst 33342 are both excited in a wavelength range that is provided by a UVB, rather than a UVA light source, which is filtered out by most materials containing foils. The transmittance of the carrier materials for the wavelength required to excite the fluorescent compound has to be considered or an illumination from the top must be possible in the imaging unit.

It was shown that DNA solutions can be left to dry on suitable carrier materials and still display their usual response to DNA dyes after renaturation, but on each material the amount of dye and DNA needed differed. For Hoechst 33342 no fitting settings were found, maybe the amounts of DNA and dye need to be higher. The YOYO-1 dye showed the greatest increase in fluorescence on the filter paper Whatman Grade 1 and the foil Hostaphan GUV 4600, with a steeper increase for higher dye concentrations. As the foil induces handling issues, the filter paper will be used in future experiments on printing an aptamer-based CFX biosensor. Future studies need to examine more material properties which play a role in immobilizing and maintaining the functionality of nucleic acids, like the surface energy. Another problem is building a detector system based on minimal fluorescence changes. Even after finding good conditions, the detected intensity was often hard or impossible to distinguish from the auto fluorescence of the DNA dye. An ideal detector system should produce a much better contrast between positive and negative probes.

References

Alocilja, E.C. and Radke, S.M., 2003. Market analysis of biosensors for food safety. *Biosensors and Bioelectronics,* 18(5–6), pp. 841–846. http://dx.doi.org/10.1016/S0956-5663(03)00009-5.

Bachmann, T.T. and Schmid, R.D., 1999. A disposable multielectrode biosensor for rapid simultaneous detection of the insecticides paraoxon and carbofuran at high resolution. *Analytica Chimica Acta,* 401(1–2), pp. 95–103. https://doi.org/10.1016/S0003-2670(99)00513-9.

Brandt, A., Gorenflo, A., Siede, R., Meixner, M. and Büchler, R., 2016. The neonicotinoids thiacloprid, imidacloprid, and clothianidin affect the immunocompetence of honey bees (Apis mellifera L.). *Journal of Insect Physiology*, 86, pp. 40–47. https://doi.org/10.1016/j.jinsphys.2016.01.001.

Carrasquilla, C., Little, J.R.L., Li, Y. and Brennan, J.D., 2015. Patterned paper sensors printed with long-chain DNA aptamers. *Chemistry,* 21(20), pp. 7369–7373. https://doi.org/10.1002/chem.201500949.

Cháfer-Pericás, C., Maquieira, Á. and Puchades, R., 2010. Fast screening methods to detect antibiotic residues in food samples. *TrAC Trends in Analytical Chemistry*, 29(9), pp. 1038–1049. https://doi.org/10.1016/j.trac.2010.06.004.

Ecker, D.J., Sampath, R., Massire, C., Blyn, L.B., Hall, T.A., Eshoo, M.W. and Hofstadler, S.A., 2008. Ibis T5000: a universal biosensor approach for microbiology. *Nature Reviews Microbiology*, 6, pp. 553–558. https://doi.org/10.1038/nrmicro1918.

Edwards, T.E., Klein, D.J. and Ferré-D'Amaré, A.R., 2007. Riboswitches: small-molecule recognition by gene regulatory RNAs. *Current Opinion in Structural Biology*, 17(3), pp. 273–279. https://doi.org/10.1016/j.sbi.2007.05.004.

Ellington, A.D. and Szostak, J.W., 1990. In vitro selection of RNA molecules that bind specific ligands. *Nature*, 346, pp. 818–822. https://doi.org/10.1038/346818a0.

Garst, A.D., Edwards, A.L. and Batey, R.T., 2011. Riboswitches: structures and mechanisms. *Cold Spring Harbor Perspectives in Biology*, 3:a003533. https://doi.org/10.1101/cshperspect.a003533.

Goldmann, T. and Gonzalez, J.S., 2000. DNA-printing: utilization of a standard inkjet printer for the transfer of nucleic acids to solid supports. *Journal of Biochemical and Biophysical Methods*, 42(3), pp. 105–110. https://doi.org/10.1016/S0165-022X(99)00049-4.

Groher, F., Bofill-Bosch, C., Schneider, C., Braun, J., Jager, S., Geißler, K., Hamacher, K. and Suess, B., 2018. Riboswitching with ciprofloxacin — development and characterization of a novel RNA regulator. *Nucleic Acids Research*, 46(4), pp. 2121–2132. https://doi.org/10.1093/nar/gkx1319.

Groher, F. and Suess, B., 2016. In vitro selection of antibiotic-binding aptamers. *Methods*, 106, pp. 42–50. https://doi.org/10.1016/j.ymeth.2016.05.008.

Hoechst, n.d. *Hoechst 33342, Trihydrochloride, Trihydrate, 100 mg*. [online] Thermo Fisher Scientific Inc. Available at: <https://www.thermofisher.com/order/catalog/product/H1399> [Accessed 30 November 2018].

Jaeger, J., Groher, F., Stamm, J., Spiehl, D., Braun, j., Dörsam, E. and Suess, B., 2019. Characterization and inkjet printing of an RNA aptamer for paper-based biosensing of coprofloxacin. *Biosensors*, 9(1). https://doi.org/10.3390/bios9010007.

Joshi, K., Chen, W., Wang, J., Schöning, M. and Mulchandani, A., 2006. Biosensors for environmental monitoring and homeland security. In: J.M. van Emon, ed. *Immunoassay and other bioanalytical techniques*. Boca Raton: CRC Press. https://doi.org/10.1201/9781420020694.

Justino, C.I.L., Duarte, A.C. and Rocha-Santos, T.A.P., 2017. Recent progress in biosensors for environmental monitoring: a review. *Sensors*, 17(12):2918. https://doi.org/10.3390/s17122918.

Kipphan, H. ed., 2001. *Handbook of print media: technologies and production methods*. Berlin: Springer-Verlag.

Kivirand, K., Kagan, M. and Rinken, T., 2013. Calibrating biosensors in flow-through set-ups: studies with glucose optrodes. In: T. Rinken, ed. *State of the art in biosensors – general aspects*. IntechOpen. https://doi.org/10.5772/45127.

McKeague, M. and DeRosa, M.C., 2012. Challenges and opportunities for small molecule aptamer development. *Journal of Nucleic Acids*, 2012:748913. http://dx.doi.org/10.1155/2012/748913.

Mello, L.D. and Kubota, L.T., 2002. Review of the use of biosensors as analytical tools in the food and drink industries. *Food Chemistry*, 77(2), pp. 237–256. https://doi.org/10.1016/S0308-8146(02)00104-8.

Mohassieb, S.A., Kirah, K., Dörsam, E., Khalil, A.S.G. and El-Hennawy, H.M., 2017. Effect of silver nanoparticle ink drop spacing on the characteristics of coplanar waveguide monopole antennas printed on flexible substrates. *IET Microwaves, Antennas & Propagation*, 11(11), pp. 1572–1577. http://dx.doi.org/10.1049/iet-map.2017.0078.

Novais, Â., Comas, I., Baquero, F., Cantón, R., Coque, T.M., Moya, A., González-Candelas, F. and Galán, J.-C., 2010. Evolutionary trajectories of beta-lactamase CTX-M-1 cluster enzymes: predicting antibiotic resistance. *PLoS Pathogens*, 6(1):e1000735. https://doi.org/10.1371/journal.ppat.1000735.

Okamoto, T., Suzuki, T. and Yamamoto, N., 2000. Microarray fabrication with covalent attachment of DNA using bubble jet technology. *Nature Biotechnology*, 18, pp. 438–441. https://doi.org/10.1038/74507.

Pankalla, S., Ganesan, R., Spiehl, D., Sauer, H.M., Dörsam, E. and Glesner, M., 2013. Mass characterisation of organic transistors and Monte-Carlo circuit simulation. *Organic Electronics*, 14(2), pp. 676–681. http://dx.doi.org/10.1016/j.orgel.2012.11.033.

Raupp, S., Daume, D., Tekoglu, S., Merklein, L., Lemmer, U., Hernandez-Sosa, G., Sauer. H.M., Dörsam, E., Scharfer, P. and Schabel, W., 2017. Slot die coated and flexo printed highly efficient SMOLEDs. *Advanced Materials Technologies*, 2(2):1600230. https://doi.org/10.1002/admt.201600230.

Song, S., Xu, H. and Fan, C., 2006. Potential diagnostic applications of biosensors: current and future directions. *International Journal of Nanomedicine*, 1(4), pp. 433–440.

Spiehl, D., Häming, M., Sauer, H.M., Bonrad, K. and Dörsam, E., 2015. Engineering of flexo- and gravure-printed indium-zinc-oxide semiconductor layers for high-performance thin-film transistors. *IEEE Trans. Electron Devices*, 62(9), pp. 2871–2877. http://dx.doi.org/10.1109/ted.2015.2449665.

Stamm, J., Spiehl, D., Jaeger, J., Groher, F., Meckel, T., Suess, B. and Dörsam, E., 2018. DNA and DNA staining as a test system for the development of an aptamer-based biosensor for sensing of antibiotics. In: P. Gane, ed. *Advances in Printing and Media Technology: Proceedings of the 45th International Research Conference of iarigai*. Warsaw, Poland, October 2018. Darmstadt, Germany: International Association of Research Organizations for the Information, Media and Graphic Arts Industries, pp. 133–142.

Threlfall, E.J., Ward, L.R., Frost, J.A. and Willshaw, G.A., 2000. The emergence and spread of antibiotic resistance in food-borne bacteria. *International Journal of Food Microbiology*, 62(1–2), pp. 1–5. https://doi.org/10.1016/S0168-1605(00)00351-2.

Ververis, C., Georghiou, K., Christodoulakis, N., Santas, P. and Santas, R., 2004. Fiber dimensions, lignin and cellulose content of various plant materials and their suitability for paper production. *Industrial Crops and Products*, 19(3), pp. 245–254. https://doi.org/10.1016/j.indcrop.2003.10.006.

Wang, C.-Y.J., Giambrone, J.J. and Smith, B.F., 2002. Detection of duck hepatitis B virus DNA on filter paper by PCR and SYBR green dye-based quantitative PCR. *Journal of Clinical Microbiology*, 40(7), pp. 2584–2590. http://dx.doi.org/10.1128/JCM.40.7.2584-2590.2002.

Wang, J., 2001. Glucose biosensors: 40 years of advances and challenges. Electroanalysis, 13(12), pp. 983–988. https://doi.org/10.1002/1521-4109(200108)13:12<983::AID-ELAN983>3.0.CO;2-%23.

Yamada, K., Henares, T.G., Suzuki, K. and Citterio, D., 2015. Paper-based inkjet-printed microfluidic analytical devices. *Angewandte Chemie*, 54(18), pp. 5294–5310. https://doi.org/10.1002/anie.201411508.

YOYO-1, n.d. *YOYO™-1 Iodide (491/509) – 1 mM Solution in DMSO*. [online] Thermo Fisher Scientific Inc. Available at: <https://www.thermofisher.com/order/catalog/product/Y3601> [Accessed 30 November 2018].